6 Models of cytoskeletal mechanics based on tensegrity

Dimitrije Stamenović

ABSTRACT: Cell shape is an important determinant of cell function and it provides a regulatory mechanism to the cell. The idea that cell contractile stress may determine cell shape stability came with the model that depicts the cell as tensed membrane that surrounds viscous cytoplasm. Ingber has further advanced this idea of the stabilizing role of the contractile stress. However, he has argued that tensed intracellular cytoskeletal lattice, rather than the cortical membrane, confirms shape stability to adherent cells. Ingber introduced a special class of tensed reticulated structures, known as tensegrity architecture, as a model of the cytoskeleton. Tensegrity architecture belongs to a class of stress-supported structures, all of which require preexisting tensile stress ("prestress") in their cable-like structural members, even before application of external loading, in order to maintain their structural integrity. Ordinary elastic materials such as rubber, polymers, or metals, by contrast, require no such prestress. A hallmark property that stems from this feature is that structural rigidity (stiffness) of the matrix is nearly proportional to the level of the prestress that it supports. As distinct from other stress-supported structures falling within the class, in tensegrity architecture the prestress in the cable network is balanced by compression of internal elements that are called struts. According to Ingber's cellular tensegrity model, cytoskeletal prestress in generated by the cell contractile machinery and by mechanical distension of the cell. This prestress is carried mainly by the cytoskeletal actin network, and is balanced partly by compression of microtubules and partly by traction at the extracellular adhesions.

The idea that the cytoskeleton maintains its structural stability through the agency of contractile stress rests on the premise that the cytoskeleton is a static network. In reality, the cytoskeleton is a dynamic network, which is exposed to dynamic loads and in which the dynamics of various biopolymers contribute to its rheological properties. Thus, the static model of the cytoskeleton provides only a limited insight into its mechanical properties (for example, near-steady-state conditions). However, our recent measurements have shown that cell rheological (dynamic) behavior may also be affected by the contractile prestress, suggesting thereby that the tensegrity idea may also account for some features of cell rheology.

This chapter describes the basic idea of the cellular tensegrity hypothesis, how it applies to problems in cellular mechanics, and what its limitations are.

Introduction

A new model of cell structure to explain how the internal cytoskeleton of adherent cells mediates alterations in cell functions caused by changes in cell shape was

proposed in the early 1980s by Donald Ingber and colleagues (Ingber et al., 1981; Ingber and Jamieson, 1985). This model is based on a building system known as *tensegrity architecture* (Fuller, 1961). The essential premise of what is known as the cellular tensegrity model is that the cytoskeletal lattice carries preexisting tensile stress, termed prestress, whose role is to confer shape stability to the cell. A second premise is that this cytoskeletal prestress is partly balanced by forces that arise at cell adhesions to the extracellular matrix and partly by internal, compression-supporting cytoskeletal structures (for example, microtubules). The cytoskeletal prestress is generated actively, by the cytoskeletal contractile apparatus. Additional prestress is generated passively by cell mechanical distension through adhesions to the substrate, by cytoplasmic swelling pressure (turgor), and by forces generated by filament polymerization. The prestress is primarily carried by the cytoskeletal actin network and to a lesser extent by the intermediate filament network (Ingber, 1993; 2003a).

There is a growing body of experimental data that is consistent with the cellular tensegrity model. The strongest piece of evidence in support of the tensegrity model is the observed proportional relationship between cell stiffness and the cytoskeletal contractile stress (Wang et al., 2001; 2002). Experimental data also show that microtubules carry compression that, in turn, balances a substantial portion of the prestress, which is another key feature of tensegrity architecture (Wang et al., 2001; Stamenović et al., 2002a). Together, these two findings have provided so far the most convincing evidence in support of the cellular tensegrity model.

In successive sections, this chapter describes basic concepts, definitions, and underlying mechanisms of the cellular tensegrity model; describes experimental data that are consistent and those that are not consistent with the tensegrity model; and describes results from mathematical modeling of typical tensegrity-based models of cell mechanics and compares predictions from those models to experimental data from living cells. Then the chapter briefly discusses the usefulness of the tensegrity idea in studying the dynamic behavior of cells and ends with a summary.

The cellular tensegrity model

It is well established that cell shape is critical for the control of many cell behaviors, including growth, motility, differentiation, and apoptosis and that the effects of cell shape are mediated through changes in the intracellular cytoskeleton (see Ingber, 2003a and 2003b). To explain how cells generate mechanical stresses in response to alterations in their shape and how those stresses affect cellular function, various models of cellular mechanics have been advanced, as other chapters here extensively discuss. All these models can be divided into two distinct classes: continuum models, and discrete models.

Continuum models (Theret et al., 1988; Evans and Yeung, 1989; Fung and Liu, 1993; Schmid-Schönbein et al., 1995; Bausch et al., 1998; Fabry et al., 2001a) assume that the stress-bearing elements within the cell are small compared to the length scales of interest and that they uniformly fill the space within the cell body. The microscale behavior of these elements is given by equations that describe local deformation and mass, and momentum and energy balance (see Chapter 3 of this book). This leads to descriptions of stress and strain patterns that are continuous in space within the cell.

Continuum models can run from simple to very complex and multicompartmental, from elastic to viscoelastic (Chapter 4) or even poroelastic (Chapter 5).

Discrete models (Porter, 1984; Ingber and Jamieson, 1985; Forgacs, 1995; Satcher and Dewey, 1996; Stamenović et al., 1996; Boey et al., 1998) consider discrete stress-bearing elements of the cell that are finite in size, sometimes spanning distances that are comparable to the cell size (for example, microtubules). The cell is depicted as being composed of a large number of these discrete elements that do not fill the space. The behavior of each discrete element is subject to conditions of mechanical equilibrium and geometrical compatibility at every node. At this point, a coarse-graining average can be applied and local stresses and strains can be obtained as continuous field variables. Within the class of discrete models there is a special subclass, known as stress-supported (or prestressed) structures. While ordinary elastic materials such as rubber, polymers, or metals, by contrast, require no such prestress, all stress-supported structures require tensile prestress in their structural members, even before the application of external loading, in order to maintain their structural integrity. A hallmark property that stems from this feature is that structural rigidity (stiffness) of the matrix is proportional to the level of the prestress that it supports (Volokh and Vilnay, 1997; Stamenović and Ingber, 2002). Tensegrity architecture falls within this class. As in the case of continuum models, discrete models, of which the tensegrity architecture is one, can range from very simple to very complex, multimodular, and multicompartmental.

It has long been known that many cell types exist under tension (prestress) (Harris et al., 1980; Albrecht-Buehler, 1987; Heidemann and Buxbaum, 1990; Kolodney and Wysolmerski, 1992; Evans et al., 1993). Theoretical models that depict the cell as a tensed (that is, prestressed) membrane that surrounds viscous cytoplasm have been proposed in the past (Evans and Yeung, 1989; Fung and Liu, 1993; Schmid-Schönbein et al., 1995). However, none of those studies show that this cell prestress may play a key role in regulating cell deformability. In the early 1980s, Donald Ingber (Ingber et al., 1981; Ingber and Jamieson, 1985) introduced a novel model of cytoskeletal mechanics based on architecture that secures structural stability through the agency of prestress. This model has become known as the cellular tensegrity model. Basic features and mechanisms of this model and how they apply to mechanics of cells are described in the coming sections.

Definitions, basic mechanisms, and properties of tensegrity structures

Tensegrity architecture is a building principle introduced by R. Buckminster Fuller (Fuller, 1961). He defined tensegrity as a system through which structures are stabilized by continuous tension carried by the structural members (like a camp tent or a spider web) rather than continuous compression (like a stone arch). Fuller referred to this architecture as "tensional integrity," or "tensegrity" (Fig. 6-1).

The central mechanism by which tensegrity and other prestressed structures develop restoring stress in the presence of external loading is by geometrical rearrangement (that is, by change in spacing and orientation and to a lesser degree by change in length) of their pre-tensed members. The greater the pre-tension carried by these members, the less geometrical rearrangement they undergo under an applied load, and thus the less deformable (more rigid) the structure will be. In the absence of prestress, these

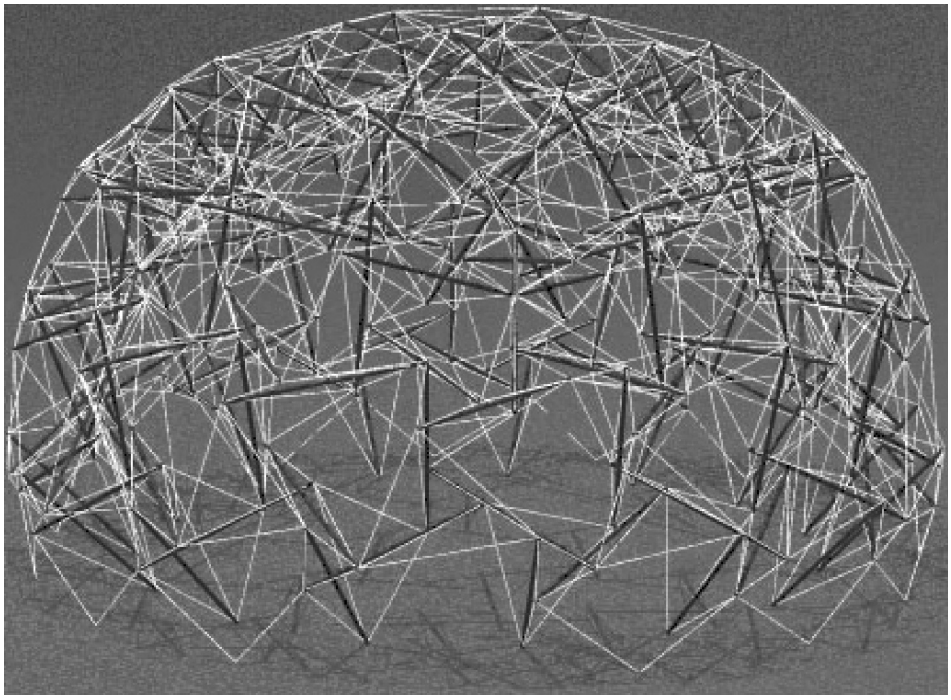

Fig. 6-1. A cable-and-strut tensegrity dome ("Dome Image ©1999 Bob Burkhardt"). In this structure, tension in the cables (white lines) is partly balanced by the compression of the struts (thick black lines) and partly by the attachments to the substrate. At each free node one strut meets several cables. Adapted with permission from Burkhardt, 2004.

structures become unstable and collapse. This explains why the structural stiffness increases in proportion with the level of the prestress.

An interesting (although not an intrinsic) property of tensegrity structures is a long-distance transfer of mechanical disturbances. Ingber referred to this phenomenon as the "action at a distance" effect (Ingber, 1993; 2003a). Because tensegrity structures resist externally applied loads by geometrical rearrangements of their structural members, any local disturbance should result in a global rearrangement of the structural lattice and should be manifested at points distal from the point of an applied load. This is quite different from continuum models where local disturbances produce only local responses, which dissipate inversely with the distance from the point of load application. In complex and multimodular tensegrity structures, this action at a distance may not be easily observable because the effect of an applied mechanical disturbance may be dissipated through the multi-connectedness of structural members and fade away at points distal from the point of load application.

The cellular tensegrity model

In the cellular tensegrity model, actin filaments and intermediate filaments of the cytoskeleton are envisioned as tensile elements (cables) that carry the prestress. Microtubules and thick cross-linked actin bundles, on the other hand, are viewed as

compression elements (struts) that partly balance the prestress. The rest of the prestress is balanced by the extracellular matrix, which is physically connected to the cytoskeleton through the focal adhesion complex. In highly spread cells, however, intracellular compression-supporting elements may become redundant and the extracellular matrix may balance the entire prestress. In other words, the cytoskeleton and the extracellular matrix are viewed as a single, synergetic, mechanically stabilized system, or the "extended cytoskeleton" (Ingber, 1993). Thus, although the cellular tensegrity model allows for the presence of internal compression-supporting elements, they are neither necessary nor sufficient for the overall stress balance in the cell–extracellular matrix system.

Do living cells behave as predicted by the tensegrity model?

This section presents a survey of experimental data that are consistent with the cellular tensegrity model, as well as those that are not.

Circumstantial evidence

Data obtained from *in vitro* biophysical measurements on isolated actin filaments (Yanagida et al., 1984; Gittes et al., 1993; MacKintosh et al., 1995) and microtubules (Gittes et al., 1993; Kurachi et al., 1995) indicate that actin filaments are semiflexible, curved, of high tensile modulus (order of 1 GPa), and of the persistence length (a measure of stiffness of a polymer molecule that can be described as a mean radius of curvature of the molecule at some temperature due to thermal fluctuations) on the order of 10 μm. On the other hand, microtubules appeared straight, as rigid tubes, of nearly the same modulus as actin filaments but of much greater persistent length, order of 10^3 μm. Based on these persistence lengths, actin filaments should appear curved and microtubules should appear straight on the whole cell level if they were not mechanically loaded. However, immunofluorescent images of the cytoskeleton lattice of living cells (Fig. 6-2) show that actin filaments appear straight, whereas microtubules appeared curved (Kaech et al., 1996; Eckes et al., 1998, 2003a). It follows, therefore, that some type of mechanical force must act on these molecular filaments in living cells: conceivably, the tension in actin filaments straighten them while compression in microtubules result in their bending (caused by buckling). On the other hand, Satcher et al. (1997) found that in endothelial cells the average pore size of the actin cytoskeleton ranges from 50–100 nm, which is much smaller than the persistence length of actin filaments. This, in turn, suggests that the straight appearance of actin cytoskeletal filaments is the result of their very short length relative to their persistence length.

It is well established that the prestress borne by the cytoskeleton is transmitted to the substrate through transmembrane integrin receptors. Harris et al. (1980) showed that in response to the contraction of fibroblasts cultured on a flexible silicon rubber substrate, the substrate wrinkles. Similarly, contracting fibroblasts that adhere to a polyacrylamide gel substrate cause the substrate to deform (Pelham and Wang, 1997). Severing focal adhesion attachments of endothelial cells to the substrate by trypsin results in a quick retraction of these cells (Sims et al., 1992), suggesting that

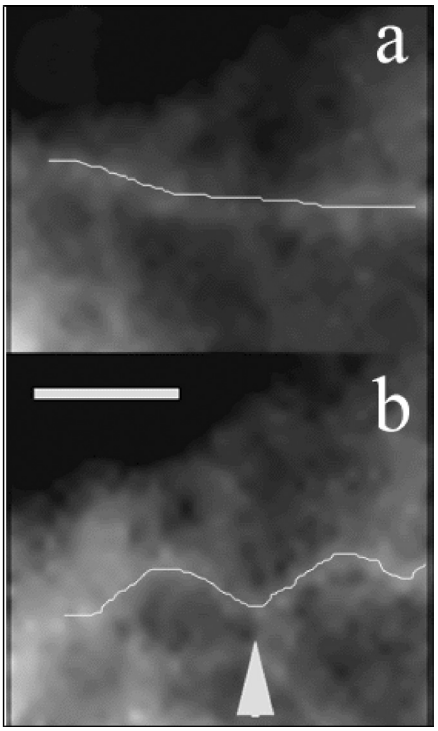

Fig. 6-2. Local buckling of a green fluorescent protein-labeled microtubule (arrowhead) in living endothelial cells following cell contraction induced by thrombin. The microtubule appears fairly straight prior to cell contraction (a) and assumes a typical sinusoidal buckled shape following contraction (b). The white lines are drawn to enhance the shape of microtubule; the scale bar is 2 μm. Adapted with permission from Wang et al., 2001.

the cytoskeleton carries prestress and that this prestress is transmitted to and balanced by traction forces that act at the cell-anchoring points to the substrate.

Experimental observations support the existence of a mechanical coupling between tension carried by the actin network and compression of microtubules, analogous to the tension-compression synergy in the cable-and-strut tensegrity model. For example, as migrating cultured epithelial cells contract, their microtubules in the lamellipodia region buckle as they resist the contractile force exerted on them by the actin network (Waterman-Storer and Salmon, 1997). Extension of a neurite, which is filled with microtubules, is opposed by pulling forces of the actin microfilaments that surround those microtubules (Heidemann and Buxbaum, 1990). Microtubules of endothelial cells, which appear straight in relaxed cells, appear buckled immediately following contraction of the actin network (Fig. 6-2) (Wang et al., 2001). In their mechanical measurements on fibroblasts, Heidemann and co-workers also observed the curved shape of microtubules. However, they associated these configurations with fluid-like behavior of microtubules because they observed slow recovery of microtubules following mechanical disturbances applied to the cell surface (Heidemann et al., 1999; Ingber et al., 2000). Contrary to these observations, Wang et al. (2001) observed relatively quick recovery of microtubules in endothelial cells following mechanical disturbances.

Cells of various types probed with different techniques exhibit a stiffening effect, such that cell stiffness increases progressively with increasingly applied mechanical load (Petersen et al., 1982; Sato et al., 1990; Alcaraz et al., 2003). This, in turn, implies that stress-strain behavior of cells is nonlinear, such that stress increases

faster than strain. This stiffening is also referred to as a strain or stress hardening. In discrete structures, this nonlinearity is primarily a result of geometrical rearrangement and recruitment of structural members in the direction of applied load, and less due to nonlinearity of individual structural members (Stamenović et al., 1996). In their early works, Ingber and colleagues considered this stiffening to be a key piece of evidence in support of the cellular tensegrity idea, as various physical (Wang et al., 1993) and mathematical (Stamenović et al., 1996; Coughlin and Stamenović, 1998) tensegrity models exhibit this behavior under certain types of loading. It turns out that this is an inconclusive piece of evidence that neither supports nor refutes the tensegrity model for the following reasons. First, the stress/strain hardening behavior characterizes various types of solid materials, many of which are not at all related to tensegrity. Second, the stress/strain hardening behavior is not an intrinsic property of tensegrity structures because they can also exhibit softening – that is, under a given loading their stiffness may decrease with increasingly applied load (Coughlin and Stamenović, 1998; Volokh et al., 2000) – or they may, under certain conditions, have constant stiffness, independent of the applied load (Stamenović et al., 1996). Third, recent mechanical measurements in living airway smooth muscle cells showed that their stress-strain behavior is linear over a wide range of applied stress, and thus they exhibit neither stiffening nor softening (Fabry et al., 1999; 2001).

Based on the above circumstantial evidence and differing interpretations of the evidence, it is clear that rigorous experimental validation of the cellular tensegrity model was needed to demonstrate a close association between cell stiffness and cytoskeletal prestress, and to show that cells exhibit the action-at-a-distance behavior. Also essential is quantitative assessment of the contribution of the substrate vs. compression of microtubules in balancing the prestress, and also understanding the role of intermediate filaments in the context of the tensegrity model. New advances in cytometry techniques made it possible to provide direct, quantitative data for these behaviors. These data are described below.

Prestress-induced stiffening

An a priori prediction of all prestressed structures is that their stiffness increases in nearly direct proportion with prestress (Volokh and Vilnay, 1997). A number of experiments in various cell types have shown evidence of prestress-induced stiffening. For example, it has been shown that mechanical (Wang and Ingber, 1994; Pourati et al., 1998; Cai et al., 1998), pharmacological (Hubmayr et al., 1996; Fabry et al., 2001), and genetic (Cai et al., 1998) modulations of cytoskeletal prestress are paralleled by changes in cell stiffness. Advances in the traction cytometry technique (Fig. 6-3) made it possible to quantitatively measure various indices of cytoskeletal prestress (Pelham and Wang, 1997; Butler et al., 2002; Wang et al., 2002). These data are then correlated with data obtained from measurements of cell stiffness. It was found (see Fig. 6-4) that in cultured human airway smooth muscle cells whose contractility was altered by graded doses of contractile and relaxant agonists, cell stiffness (G) increases in direct proportion with the contractile stress (P); $G \approx 1.04P$ (Wang et al., 2001; 2002). Although this association between cell stiffness and contractile stress does not preclude other interpretations, it is the hallmark of structures that secure

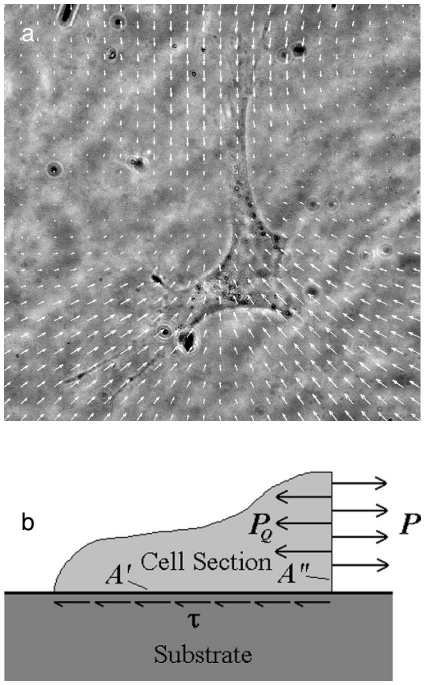

Fig. 6-3. (a) A human airway smooth muscle cell cultured on a flexible polyacrylamide gel substrate. As the cell contracts (histamine 10 μM), the substrate deforms, causing fluorescent microbead markers embedded in the gel to move (arrows). From measured displacement field of the markers and known elastic properties of the gel, one can calculate traction (τ) that arises at the cell-gel interface (Butler et al., 2002). Because the cytoskeletal prestress (P) is balanced partly by τ, one can asses P(Wang et al., 2002). (b) A free body diagram of a cell section depicting a three-way force balance between the cytoskeleton (P), substrate (P_S), and microtubules (P_Q): $P_S = P - P_Q$ where P_S indicates the part of P that is balanced by the substrate and P_Q indicates the part of P that is balanced by compression-supporting microtubules. At equilibrium, the force balance requires that $\tau A' = P_S A''$ where A' and A'' are interfacial and cross-sectional areas of the cell section, respectively. Because τ, A' and A'' can be directly measured, one can obtain P_S. A' and A'' were measured for many optical cross-sections of the cell. For each section, P_S was calculated and the average value was obtained (Wang et al., 2002). Note that in the absence of internal compression structures (for example, upon disruption of microtubules), $P_Q = 0$ and the entire prestress P is balanced by τ (i.e., $P_S = P$).

shape stability through the agency of the prestress. Other possible interpretations of this finding are discussed below.

In addition to generating contractile force, it has been shown that pharmacological agonists also induce polymerization of the actin network (Mehta and Gunst, 1999; Tang et al., 1999). Thus, the observed stiffening in response to contractile agonists could be nothing more than the result of actin polymerization. However, An et al. (2002) have shown that agonist-induced actin polymerization in smooth muscle cells accounts only for a portion of the observed stiffening, whereas the remaining portion of the stiffening is associated with contractile force generation. Another potential mechanism that could explain the data in Fig. 6-4 is the effect of cross-bridge recruitment. It is known from studies of isolated smooth muscle strips in uniaxial extension that both muscle stiffness and muscle force are directly proportional to the number of attached cross-bridges (Fredberg et al., 1996). Thus, the proportionality between the cell stiffness and the prestress could reflect nothing more than the effect of changes in the number of attached cross-bridges in response to pharmacological stimulation. A result that goes against this possibility is obtained from a theoretical model of the myosin cross-bridge kinetics (Mijailovich et al., 2000). This model predicts a qualitatively different oscillatory response from the one measured in airway smooth muscle cells (Fabry et al., 2001). Thus, the kinetics of cross-bridges cannot explain all aspects of cytoskeletal mechanics.

Action at a distance

To investigate whether the cytoskeleton exhibits the action-at-a-distance effect, Maniotis et al. (1997) performed experiments in which the tip of a glass micropipette

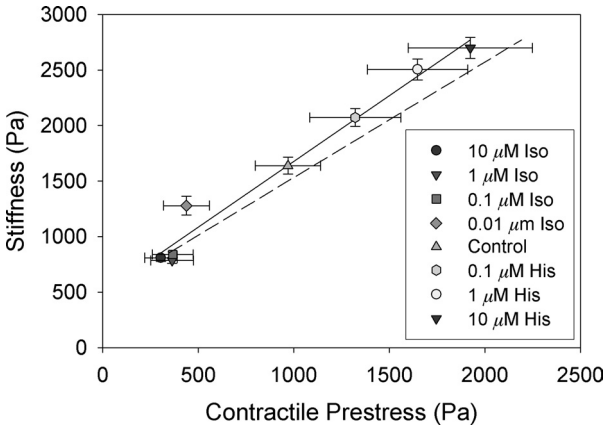

Fig. 6-4. Cell stiffness (G) increases linearly with increasing cytoskeletal contractile stress. Measurements were done in cultured human airway smooth muscle cells. Cell contractility was modulated by graded doses of histamine (constrictor) and graded doses of isoproterenol (relaxant). Stiffness was measured using the magnetic cytometry technique and the prestress was measured by the traction cytometry technique (Wang et al., 2002). The slope of the regression line is 1.18 (solid line). The measured prestress represents the portion of the cytoskeletal prestress that is balanced by the substrate (that is, P_S from Fig. 6-3). Because in those cells microtubules balance on average ∼14% of P_S (Stamenović et al., 2002a), the slope of the stiffness vs. the total prestress (P) relationship should be reduced by 14% and thus equals 1.04 (dashed line). The stiffness vs. prestress relationship displays a nonzero intercept. This is due to a bias in the method used to calculate the prestress (in other words, the cell cross-sectional area A'' from Fig. 6-3 is an overestimate) (Wang et al., 2002). In the absence of this artifact, the stiffness vs. prestress relationship would display close-to-zero intercept, that is, $G \approx 1.04P$ (Wang et al., 2002). (Redrawn from Wang et al. (2002) and Stamenović et al. (2002b); G is rescaled to take into account the effect of bead internalization. From Mijailovich et al., 2002.

coated with fibronectin and bound to integrin receptors of living endothelial cells was pulled laterally. Because integrins are physically linked to the cytoskeleton, then if the cytoskeleton is organized as a discrete tensegrity structure, pulling on integrins should produce an observable deformation distal from the point of load application. The authors observed that the nuclear border moved along the line of applied pulling force, which is a manifestation of the action at a distance. A more convincing piece of evidence for this phenomenon was provided by Hu et al. (2003). These investigators designed the intracellular tomography technique that enabled them to observe displacement distribution within the cytoskeleton region in response to locally applied shear disturbance. Lumps of displacement concentrations were found at distances greater than 20 μm from the point of application of the shear loading, which is indicative of the action-at-a-distance effect (Fig. 6-5). Interestingly, when the actin lattice was disrupted (cytochalasin D), the action-at-a-distance effect disappeared (data not shown), suggesting that connectivity of the actin network is essential for transmission of mechanical signals throughout the cytoskeleton. The action-at-a-distance effect has also been observed in neurons (Ingber et al., 2000) and in endothelial cells (Helmke et al., 2003). On the other hand, Heidemann et al. (1999) failed to observe this phenomenon in living fibroblasts when they applied various mechanical disturbances by a glass micropipette to the cell surface through integrin receptors. They found that

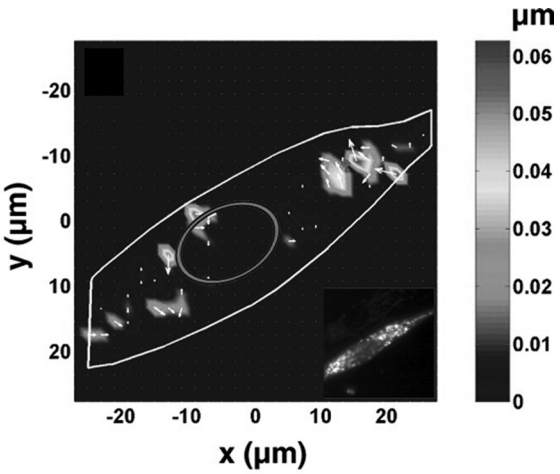

Fig. 6-5. Evidence of the action-at-a-distance effect. Displacement map in living human airway smooth muscle cells obtained using the intracellular tomography technique (Hu et al., 2003). Load is applied to the cell by twisting a ferromagnetic bead bound to integrin receptors on the cell apical surface. The bead position is shown on the phase-contrast image of the cell (inset), the black dot on the image is the bead. The white arrows indicate the direction of the displacement field and the gray-scale map represents its magnitude. Displacements do not decay quickly away from the bead center. Appreciable "lumps" of displacement concentration could be seen at distances more than 20 μm from the bead, consistent with the action-at-a-distance effect. The inner elliptical contour indicates the position of the nucleus. Adapted with permission from Hu et al., 2003.

such disturbances produced only local deformations. However, the authors did not confirm formation of focal adhesions at points of application of external loading, which is essential for load transfer between cell surface and the interior cytoskeleton (Ingber et al., 2000). Thus, their results remain controversial.

Do microtubules carry compression?

Microscopic visualization of green fluorescent protein-labeled microtubules of living cells (see Fig. 6-2) shows that microtubules buckle as they oppose contraction of the actin network (Waterman-Storer and Salmon, 1997; Wang et al., 2001). It was not known, however, whether the compression that causes this buckling could balance a substantial fraction of the contractile prestress. To investigate this possibility, an energetic analysis of buckling of microtubules was carried out (Stamenović et al., 2002a). The assumption was that energy stored in microtubules during compression was transferred to a flexible substrate upon disruption of microtubules. Thus, measurement of an increase in elastic energy of the substrate following disruption of microtubules should indicate compression energy stored in microtubules prior to their disruption. Elastic energy stored in the substrate was obtained from traction microscopy measurements as a work done by traction forces during cell contraction. It was found in highly stimulated and spread human airway smooth muscle cells that

following disruption of microtubules by colchicine, the work of traction increases on average by ∼30 percent relative to the state before disruption, and equals 0.13 pJ (Stamenović et al., 2002a). This result was then utilized in the energetic analysis. Based on the model of Brodland and Gordon (1990), the microtubules were assumed as slender elastic rods laterally supported by intermediate filaments. Using the post-buckling equilibrium theory of Euler struts (Timoshenko and Gere, 1988), the energy stored during buckling of microtubules was estimated as ∼0.18 pJ, which is close to the measured value of ∼0.13 pJ (Stamenović et al., 2002a). This is further evidence in support of the idea that microtubules are intracellular compression-bearing elements. Potential concerns are that disruption of microtubules may activate myosin light-chain phosphorylation (Kolodney and Elson, 1995) or could cause a release of intracellular calcium (Paul et al., 2000). Thus, the observed increase in traction and work of traction following disruption of microtubules could be due entirely to chemical mechanisms rather than through mechanical load transfer. These concerns are alleviated by observations indicating that microtubule disruption results in an increase of traction even when the level of myosin light-chain phosphorylation and the level of calcium do not change (Wang et al., 2001; Stamenović et al., 2002a).

From the same experimental data used in the energetic analysis, the contribution of microtubules to balancing the prestress was obtained as follows (Wang et al., 2001; Stamenović et al., 2002a). An increase in traction following microtubule disruption indicates the part of the prestress balanced by microtubules that is transferred to the substrate (see Fig. 6-3b). It was found that this increase ranges from ∼5–30 percent, depending on the cell, and is on average ∼14 percent, suggesting that microtubules balance only a small fraction of the cytoskeletal prestress and that the substrate balances the bulk of it (Stamenović et al., 2002a). An increase in traction in the response to disruption of microtubules had been observed previously, in different cell types, by other investigators, but has not been quantified (Kolodney and Wysolmersky, 1992; Kolodney and Elson, 1995). More recently, Hu et al. (2004) showed that the contribution of microtubules to balancing the prestress and to the energy budget of the cell depends on the extent of cell spreading. Using the traction cytometry technique, these investigators found that in airway smooth muscle cells, changes in traction and the substrate energy following disruption of microtubules decrease with increasing cell spreading. For example, as the cell projected area increases from 500 to 1800 μm^2, the percent increase in traction following disruption of microtubules decreases from 80 percent to a very small percent. Because in their natural habitat cells seldom exhibit highly spread forms, the above results suggest that the contribution of microtubules in balancing the prestress cannot be overlooked.

The role of intermediate filaments

Cytoskeletal-based intermediate filaments also carry prestress and link the nucleus to the cell surface and the cytoskeleton (Ingber, 1993; 2003a). In support of this view, vimentin-deficient fibroblasts were found to exhibit reduced contractility and reduced traction on the substrate in comparison to the wild-type cells (Eckes et al., 1998). Also, it was observed that the intermediate filament network alone is sufficient

to transfer mechanical load from cell surface to the nucleus in cells in which the actin and microtubule networks are chemically disrupted (Maniotis et al., 1997). Taken together, these observations suggest that intermediate filaments play a role in transferring the contractile prestress to the substrate and in long-distance load transfer within the cytoskeleton. Both are key features of the cellular tensegrity model. In addition, inhibition of intermediate filaments causes a decrease in cell stiffness (Wang et al., 1993; Eckes et al., 1998; Wang and Stamenović, 2000), as well as cytoplasmic tearing in response to high applied strains (Maniotis et al., 1997; Eckes et al., 1998). In fact, it appears that the intermediate filaments' contribution to a cell's resistance to shape distortion is substantial only at relatively large strains (Wang and Stamenović, 2000). Another role of intermediate filaments is suggested by Brodland and Gordon (1990). According to these authors, intermediate filaments provide a lateral stabilizing support to microtubules as they buckle while opposing contractile forces transmitted by the cytoskeletal actin lattice. This description is consistent with experimental data (Stamenović et al., 2002a).

Summary

Results from experimental measurements on living adherent cells indicate that their behavior is consistent with the cellular tensegrity model. It was found that cell stiffness increases directly proportionally with increasing contractile stress. It was also found that microtubules carry compression that, in turn, balances a substantial portion of the cytoskeletal prestress. This contribution of microtubules is much smaller in highly spread cells, roughly a few percent, whereas in poorly spread cells it can be as high as ∼50 percent. The majority of data from measurements of the action-at-a-distance phenomenon indicate that cells exhibit this type of behavior when the force is applied through integrin receptors at the cell surface and focal adhesions were formed at the site of force application. Intermediate filaments appear to be important contributors to cell contractility and thus to supporting the prestress. They serve as molecular "guy wires" that facilitate transfer of mechanical loads between the cell surface and the nucleus. Finally, intermediate filaments appear to stabilize microtubules as the latter balance the cytoskeletal prestress. Taken together, these observations provide strong evidence in support of the cellular tensegrity model. Although they can have alternative interpretations, there is no single model other than tensegrity that can explain all these data together.

Examples of mathematical models of the cytoskeleton based on tensegrity

Despite its geometric complexity, its dynamic nature, and its inelastic properties, the cytoskeleton is often modeled as a static, elastic, isotropic, and homogeneous network of idealized geometry. The idea is that if the mechanisms by which such an idealized model develops mechanical stress are indeed embodied within the cytoskeleton, then, despite all simplifications, the model should be able to capture key features that characterize mechanical behavior of cells under the steady-state. With the tensegrity model, however, each element is individually taken into account for a discrete formulation of the model. This section describes three types of prestressed structures that have been commonly used as models of cellular mechanics: the cortical membrane

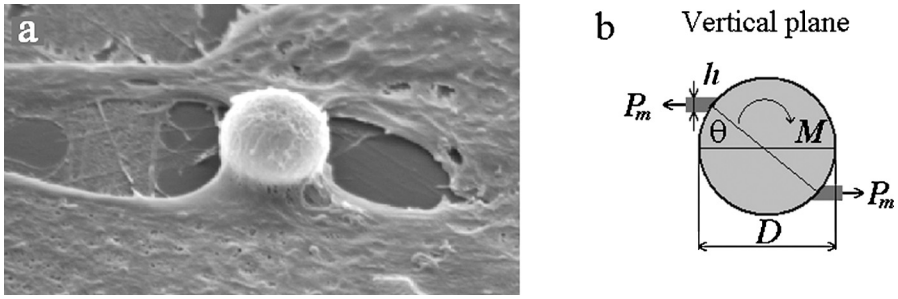

Fig. 6-6. (a) Ferromagnetic beads bound to the apical surface of cultured human airway smooth muscle cells (unpublished data kindly supplied by Dr. B. Fabry). (b) A free-body diagram of a magnetic bead of diameter D half embedded into an elastic membrane of thickness h. The bead is rotated in a vertical plane by specific torque M through angle θ. The rotation is resisted by the membrane tension (prestress) (P_m).

model; the tensed cable net model; and the cable-and-strut model. All three models are stabilized by the prestress. They differ from each other in their topological and structural organization, and in the manner by which they balance the prestress. Results obtained from the models are compared with data from living cells.

The cortical membrane model

This model assumes that the main force-bearing elements of the cytoskeleton are confined either within a thin (∼100 nm) cortical layer (Zhelev et al., 1994) or several distinct layers (Heidemann et al., 1999). The cortical layer is under sustained tension (that is, prestress) that is either entirely balanced by the pressurized cytoplasm in suspended cells, or balanced partly by the cytoplasmic pressure and partly by traction at the extracellular adhesions in adherent cells. This model has been successful in describing mechanical features of various suspended cells (Evans and Yeung, 1989; Zhelev et al., 1994; Discher et al., 1998). However, in the case of adherent cells, this model has enjoyed limited success (Fung and Liu, 1993; Schmid-Schönbein et al., 1995; Coughlin and Stamenović, 2003). To illustrate the usefulness of this model, a simulation of a magnetic twisting cytometry measurement is described below (Stamenović and Ingber, 2002).

In the magnetic twisting cytometry technique, small ferromagnetic beads (4.5-μm diameter) bound to integrin receptors on the apical surface of an adherent cell are twisted by a magnetic field, as shown in Fig. 6-6a. Because integrins are physically linked to the cytoskeleton, twisting of the bead is resisted by restoring forces of the cytoskeleton. Using the cortical membrane model, magnetic twisting measurements are simulated as follows.

A rigid spherical bead of diameter D is half-embedded in an initially tensed (prestressed) membrane of thickness h. A twisting torque (M) is applied to the bead in the vertical plane (Fig. 6-6b). Rotation of the bead is impeded by the prestress (P_m) in the membrane. By considering mechanical balance between M and P_m it was found (Stamenović and Ingber, 2002) that

$$M = D^2 P_m h \sin\theta, \tag{6.1}$$

where θ is the angle of bead rotation. In magnetic twisting measurements, a scale for the applied shear stress (T) is defined as the ratio of M and 6 times bead volume,

where 6 is the shape factor, and shear stiffness (G) as the ratio of T and θ (Wang et al., 1993; Wang and Ingber, 1994). Thus it follows from Eq. 6.1 that

$$G = \frac{1}{\pi} P_m \frac{h}{D} \frac{\sin\theta}{\theta}. \tag{6.2}$$

In the limit of $\theta \to 0$, $G \to (1/\pi)P_m(h/D)$ and represents the shear modulus of Hookean elasticity. It follows from Eq. 6.2 that G increases in direct proportion with P_m, a feature consistent with the behavior observed in living cells during magnetic twisting measurements (see Fig. 6-4). Taking into account experimentally based values for $h = 0.1$ μm, $D = 4.5$ μm, and $P_m = O(10^4{-}10^5)$ Pa it follows from Eq. 6.2 that $G = O(10^2{-}10^3)$ Pa, which is consistent with experimentally obtained values for G (see Fig. 6-4). [P_m was estimated as follows. It scales with the cytoskeletal prestress P as the ratio of cell radius R to membrane thickness h. Experimental data show that $P = O(10^2{-}10^3)$ Pa (Fig. 6-4), $R = O(10^1)$ μm and $h = O(10^{-1})$ μm, thus $P_m = O(10^4{-}10^5)$ Pa.]

Despite this agreement, several aspects of this model are not consistent with experimental results. First, Eq. 6.2 predicts that G decreases with increasing angular strain θ, in other words, softening behavior, whereas magnetic twisting measurements show stress hardening (Wang et al., 1993) or constant stiffness (Fabry et al., 2001). Second, Eq. 6.3 predicts that G decreases with increasing bead diameter D, whereas experiments on cultured endothelial cells show the opposite trend (Wang and Ingber, 1994). One reason for these discrepancies could be the assumption that the cortical layer is a membrane that carries only tensile force. In reality, the cortical layer can support bending, for example in red-blood cells (Evans, 1983; Fung, 1993), and hence a more appropriate model may be a shell-like rather than a membrane-like structure. Regardless, the assumption that the cytoskeleton is confined within a thin cortical layer that surrounds liquid cytoplasm contradicts observations in adherent cells that mechanical perturbations applied to the cell surfaces are transmitted deep into the cytoplasmic domain (Maniotis et al., 1997; Wang et al., 2001; Hu et al., 2003). These observations suggest that mechanical force transmission through the cell is facilitated through the molecular connectivity of the intracellular solid-state cytoskeletal lattice. Taken together, these inconsistencies lower our enthusiasm for the cortical-membrane model as an adequate depiction of the mechanics of adherent cells. However, it remains a good mechanical model for suspended cells where the cytoskeleton appears to be organized within a thin cortical membrane (Bray et al., 1986).

Tensed cable nets

These are reticulated networks comprised entirely of tensile cable elements (Volokh and Vilnay, 1997). Because cables do not support compression, they need to carry initial tension to prevent their buckling and subsequent collapse in the presence of externally applied load. This initial tension defines prestress that is balanced externally (for example, by attachment to the extracellular matrix), and/or internally (such as, by cytoplasmic swelling). A simple illustration of key features of tensed cable nets can be obtained by using the affine network model. A key premise of such a model is that local strains follow the macroscopic (continuum) strain field. (This assumption is

known as the affine approximation.) Using this approach and assuming that initially all cable orientations in the network are equally probable, one can obtain that the shear modulus (G) (Stamenović, 2005) is

$$G = (0.8 + 0.2B)\,P \tag{6.3}$$

where P is the prestress, $B \equiv (dF/dL)/(F/L)$ is nondimensional cable stiffness, and the F vs. L dependence represents the cable tension-length characteristsic (Budiansky and Kimmel, 1987). In general, B may depend on the level of cable tension (that is, on P). In that case, according to Eq. 6.3, the G vs. P relationship is nonlinear. If, however, B is constant, then G is directly proportional to P. The first term on the right-hand side of Eq. 6.3 represents the sum of the contributions of changes in spacing and orientation of the cables ($0.5P + 0.3P$) to G, whereas the second term ($0.2BP$) is the contribution of the lengthening of the cables to G.

To test whether the prediction of Eq. 6.3 is quantitatively consistent with experimental data from living cells (see Fig. 6-4), we estimate B from measurements of force-extension properties of isolated acto-myosin interactions (Ishijima et al., 1996). Based on these measurements, $(dF/dL)/F = 0.024\,\text{nm}^{-1}$ for a wide range of F. Thus, for a 100-nm long actin filament $B = 2.4$. The choice of filament length of $L = 100$ nm is based on the observation of the average pore-size of the actin cytoskeletal network of endothelial cells (Satcher et al., 1997). By substituting this value into Eq. 6.3, it follows that $G = 1.28P$. This is a modest overestimate of the experimentally obtained result $G = 1.04P$ (Fig. 6-4).

The most favorable aspect of this model is that it provides a mathematically transparent insight into mechanisms that may determine cytoskeletal deformability; G is primarily determined by P through change in spacing and orientation of the cable elements, and to a lesser extent by their stiffness. The model can also provide a reasonably good quantitative correspondence to experimental G vs. P data. The latter is obtained under the crude assumptions of the affine strain approximation and of equally probable distribution of cable orientations. These assumptions are known to lead toward an overestimate of G (Stamenović, 1990). The model also assumes a homogeneous distribution of the prestress throughout the cytoskeleton, although measurements show that the prestress is greatest near the cell edges and decreases toward the nuclear region (Tolić-Nørrelykke et al., 2002). However, in the experimental data for the G vs. P relationship (Fig. 6-4), P represents the mean value of the prestress distribution throughout the cell, and thus the model assumption of uniform prestress is reasonable. The model focuses only on the contribution of the actin network and ignores potential contributions of other components of the cytoskeleton. These contributions will be considered shortly. Nevertheless, the model provides a reasonably good prediction of the G vs. P relationship suggesting that the tensed actin network plays a major role in determining cell mechanical properties. The model also describes the cytoskeleton as a static, elastic network, whereas the cytoskeleton is a dynamic and inelastic structure. This issue is discussed in the section on tensegrity and cellular dynamics.

It is noteworthy that two-dimensional cable nets also have been used to model the cortical membrane. In those models the cortical membrane has been depicted as a two-dimensional network of triangles (Boey et al., 1998) and hexagons (Coughlin

and Stamenović, 2003). In the case of suspended cells, this model provides very good correspondence to experimental data. For example, the model of the spectrin lattice successfully describes the behavior of red blood cells during micropipette aspiration measurements (Discher et al., 1998). However, in the case of adherent cells, the model of the actin cortical lattice has enjoyed only moderate success. While it provides a reasonably good correspondence to data from cell poking measurements, it exhibits only some qualitative features of the cell response to twisting and pulling of magnetic beads bound to integrin receptors (Coughlin and Stamenović, 2003). Taken together, the above results show that the two-dimensional cable net model is incomplete to describe mechanical behavior of adherent cells; however the results also show that prestress is a key determinant of the model response.

Cable-and-strut model

This is a cable net model in which the prestress in the cables is balanced by internal compression-supporting struts rather than by inflating pressure. At each free node, one strut meets several cables (see Fig. 6-1). Cables carry initial tension that is balanced by compression of the strut. Together, cables and struts form a self-equilibrated and stable form in the space. This structure may also be attached to the substrate (Fig. 6-1). In this case, the anchoring forces of the substrate also contribute to the balance of tension in the cables. The main difference between these structures and the cable nets is that in the former, the struts directly contribute to the structure's resistance to shape distortion, whereas in the latter this contribution does not exist.

The shear modulus (G) of the cable and strut model can be also obtained using the affine network approach, as in the case of the tensed cable net model. It was found (Stamenović, 2005) that

$$G = 0.8(P - P_Q) + 0.2(BP + B_Q P_Q) \tag{6.4}$$

where P is the prestress carried by the cables and P_Q is the portion of P balanced by the struts, $B \equiv (dF/dL)/(F/L)$ is the nondimensional cable stiffness and $B_Q \equiv (dQ/dl)/(Q/l)$ is the nondimensional strut stiffness. The difference $P - P_Q$ represents the portion of P transmitted to and balanced by the substrate and is denoted by P_S (see Fig. 6-2b). It is this P_S that can be directly measured using the traction microscopy technique (Wang et al., 2002).

It was shown in the section on tensed cable nets that $B = 2.4$. The quantity B_Q is determined based on the buckling behavior of microtubules (Stamenović et al., 2002a). It is found that $B_Q \approx 0.54$. By substituting this value and $B = 2.4$ into Eq. 6.4 and taking into account that in well-spread smooth muscle cells, microtubules balance on average ~14 percent of P_S, that is, $P_Q = 0.14P_S$ (Stamenović et al., 2002a), it is obtained that $G = 1.19P$, which is close to the experimental data of $G = 1.04P$ (Fig. 6-4).

It is noteworthy that if $P_Q = 0$, for example, in a case where microtubules are disrupted, Eq. 6.4 reduces to Eq. 6.3. If disruption of microtubules would not affect P, then according to Eqs. 6.3 and 6.4, for a given P, the shear modulus G would be ~8 percent lower in the case of intact microtubules than in the case of disrupted microtubules. In reality, such conditions in cells are hard to achieve. An experimental

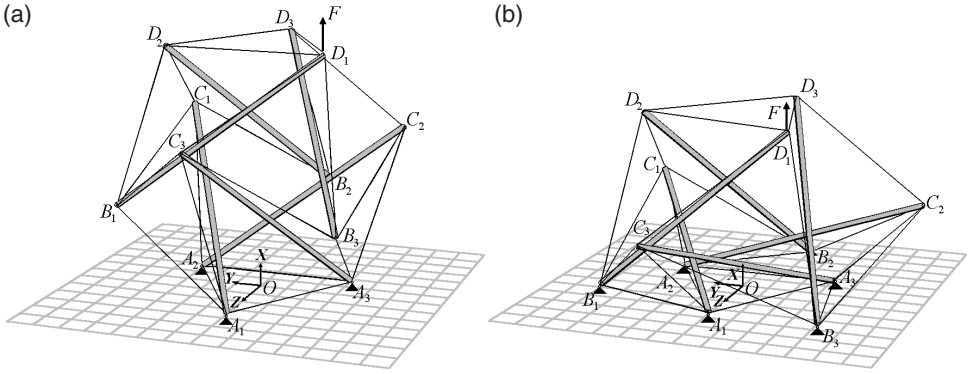

Fig. 6-7. Six-strut tensegrity model in the round (a) and spread (b) configurations anchored to the substrate. Anchoring nodes A_1, A_2 and A_3 (round) and A_1, A_2, A_3, B_1, B_2, and B_3 (spread) are indicated by solid triangles. Pulling force F (thick arrow) is applied at node D_1. Reprinted with permission from Coughlin and Stamenović, 1998.

condition that comes close to this occurs in airway smooth muscle cells stimulated by a saturated dose of histamine (10 μM). In those cells the level of prestress was maintained constant prior to and after disruption of microtubules by colchicine (Wang et al., 2001; 2002). It was found that disruption of microtubules causes a small (∼10 percent), but not significant, increase in cell stiffness (Stamenović et al., 2002b), which is close to the predicted value of ∼8 percent. On the other hand, in nonstimulated endothelial cells, disruption of microtubules causes a significant (∼20 percent) decrease in cell stiffness (Wang et al., 1993; Wang, 1998), which is opposite from the model prediction. A possible reason for this decrease in stiffness in endothelial cells is that in the absence of compression-supporting microtubules, cytoskeletal prestress in those cells decreased, and consequently the cytoskeletal lattice became more compliant.

Most of the criticism for the cable net model also applies to the cable-and-strut model. However, the ability of the model to predict the G vs. P relationship as well as the mechanical role of cytoskeleton-based microtubules such that they are consistent with corresponding experimental data, suggests that the model has captured the basic mechanisms by which the cytoskeleton resists shape distortion.

Consider next an application of a so-called six-strut tensegrity model to study the effect of cell spreading on cell deformability (Coughlin and Stamenović, 1998). This particular model has been frequently used in studies of cytoskeletal mechanics (Ingber, 1993; Stamenović et al., 1996; Coughlin and Stamenović, 1998; Volokh et al., 2000; Wang and Stamenović, 2000; Wendling et al., 1999). It is comprised of six struts interconnected with twenty-four cables (see Fig. 6-7). Although this model represents a gross oversimplification of cytoskeletal architecture, surprisingly it has provided good predictions and simulations of various mechanical behaviors observed in living cells, suggesting that it embodies key mechanisms that determine cytoskeleton mechanics.

In the six-strut tensegrity model, the struts are viewed as slender bars that support no lateral load. Initially, the cables are under tension balanced entirely by compression

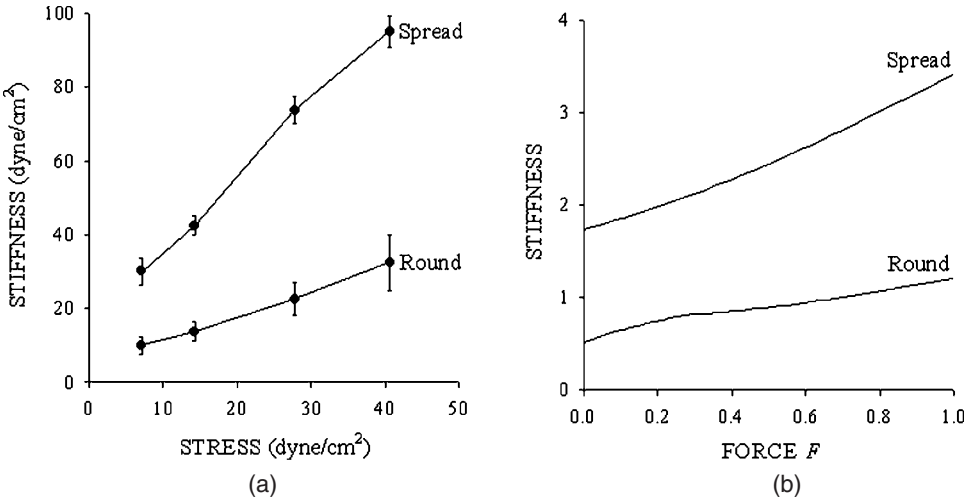

Fig. 6-8. (a) Data for stiffness vs. applied stress in round and spread cultured endothelial cells measured by magnetic twisting cytometry; points means ± SE ($n = 3$ wells, 20,000 cells/well). Both configurations exhibit stress-hardening behavior with greater hardening in the spread than in the round configuration. (Adapted with permission from Wang and Ingber (1994).) (b) Simulations of stiffness vs. applied force (F) in spread and round configurations of the six-strut model (Fig. 6-7) are qualitatively consistent with the data in panel (a). The force is given in the unit of force and the stiffness in the unit of force/length. Adapted with permission from Coughlin and Stamenović, 1998.

of the struts. The structure is then attached to a rigid substrate at three nodes through frictionless ball-joint connections (Fig. 6-7a). The initial force distribution within the structure is not affected by this attachment. This is referred to as a 'round configuration.' To mimic cell spreading, three additional nodes are also anchored to the substrate (Fig. 6-7b). This is referred to as a 'spread configuration.' As a consequence of spreading, force distribution is altered from the one in the round configuration. Tension in the cables is now partly balanced by the struts and partly by reaction forces at the anchoring nodes. In both spread and round configurations, a vertical pulling force (F) is applied at a node distal from the substrate (Fig. 6-7). The corresponding vertical displacement (Δx) is calculated and the structural stiffness as $G = F/\Delta x$. Two cases were considered, one where struts are rigid and cables linearly elastic, and the other where both struts and cables are elastic and struts buckle under compression. Here we present results from the case with rigid struts; corresponding results obtained with buckling struts are qualitatively similar (Coughlin and Stamenović, 1998). The model predicts that stiffness increases with spreading (Fig. 6-8b). The reason is that tension (prestress) in the cables increases with spreading. The model also predicts approximately linear stress-hardening behavior and predicts that this dependence is greater in the spread than in the round configuration (Fig. 6-8b). All these predictions are consistent (Fig. 6-8a) with the corresponding behavior in round and in spread endothelial cells (Wang and Ingber, 1994). Further attachments of the nodes to the substrate, that is, further spreading, would gradually eliminate the struts from the force balance scheme and their role will be taken over by the substrate.

Taken together, the above results indicate that the cable-and-strut model provides a good and plausible description of cytoskeletal mechanics. It reiterates the central role of cytoskeletal prestress in cell deformability. The cable-and-strut model also reveals the potential contribution of microtubules; they balance a fraction of the prestress, and their deformability (buckling) contributes to the overall deformability of the cytoskeleton. This contribution decreases as cell spreading increases.

In all of the above considerations, intermediate filaments are viewed only as a stabilizing support during buckling of microtubules. To investigate their contribution to cytoskeletal mechanics as stress-bearing members, elastic cables that connect the nodes of the six-strut tensegrity model with its geometric center are added to the model (Wang and Stamenović, 2000). This was based on the observed role of intermediate filaments as "guy wires" between the cell surface and the nucleus (Maniotis et al., 1997). It was shown that by including those cable members in the six-strut model, the model can account for the observed difference in the stress-strain behavior measured by magnetic twisting cytometry between normal cells and cells in which intermediate filaments were inhibited (Wang and Stamenović, 2000).

Summary

Mathematical descriptions of standard tensegrity models of cellular mechanics provide insight into how the cytoskeletal prestress determines cell deformability. Three key mechanisms through which the prestress secures shape stability of the cytoskeleton are changes in spacing, orientation, and length of structural members of the cytoskeleton. Importantly, these mechanisms are not tied to the manner by which the cytoskeletal prestress is balanced. This, in turn, implies that the close association between cell stiffness and the cytoskeletal prestress is a common characteristic of all prestressed structures. Quantitatively, however, this relationship does depend on the architectural organization of the cytoskeletal lattice, including the manner in which the prestress is balanced. The cable-and-strut model shows that in highly spread cells, where virtually the entire prestress is balanced by the substrate, the contribution of microtubules to deformability of the cytoskeleton is negligible. In less-spread cells, however, where the contribution of internal compression members to balancing the prestress increases at the expense of the substrate, deformability of microtubules importantly contributes to the overall lattice deformability. Thus, which of the three models would be appropriate to describe mechanical behavior of a cell would depend upon the cell type and the extent of cell spreading.

Tensegrity and cellular dynamics

In previous sections it was shown how tensegrity-based models could account for static elastic behavior of cells. However, cells are known to exhibit time- and rate-of-deformation-dependent viscoelastic behavior (Petersen et al., 1982; Evans and Yeung, 1989; Sato et al., 1990; Wang and Ingber, 1994; Bausch et al., 1998; Fabry et al., 2001). Because in their natural habitat cells are often exposed to dynamic loads (for example, pulsatile blood flow in vascular endothelial cells, periodic stretching of the extracellular matrix in various pulmonary adherent cells), their viscoelastic properties

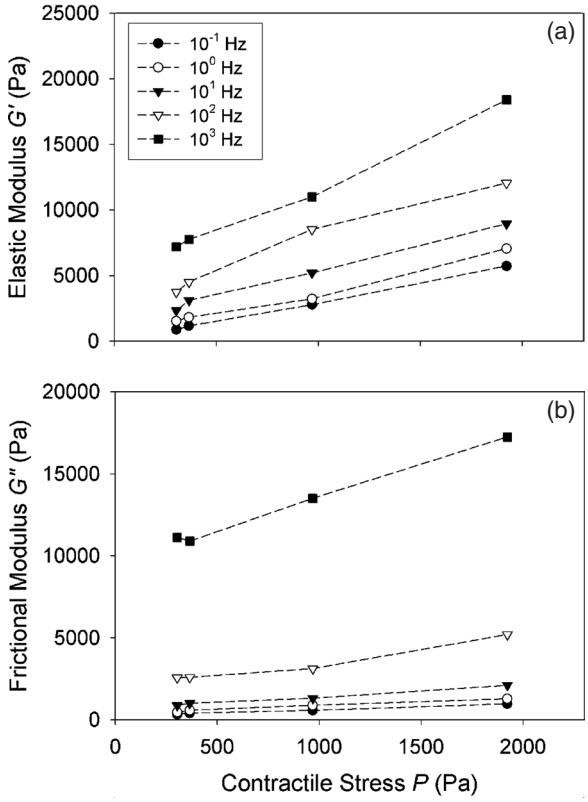

Fig. 6-9. (a) For a given frequency of loading (ω), the storage (elastic) modulus (G') increases with increasing cytoskeletal contractile prestress (P) at all frequencies. (b) The loss (viscous) modulus (G'') also increased with P at all frequencies. Cell contractility was modulated by histamine and isoproterenol. P was measured by traction cytometry and G' and G'' by magnetic oscillatory cytometry. Data are means ± SE. Adapted with permission from Stamenović et al., 2004.

are important determinants of their mechanical behavior. As the tensegrity-based models have provided a reasonably good description of elastic behavior of adherent cells, it is of considerable interest to investigate whether these models can be extended to describe viscoelastic cell behavior.

Recent oscillatory measurements on cultured airway smooth muscle cells indicate that the cytoskeletal prestress may play an important role in determining cell dynamics. It was found (see Fig. 6-9) that the cell dynamic modulus (G^*) is systematically altered in response to modulations of cell contractility; at a given frequency, the real and imaginary components of G^* – the storage (elastic) modulus (G') and loss (viscous) modulus (G''), respectively – increase with increasing contractile prestress P (Stamenović et al., 2002b; 2004). These prestress-dependences of G' and G'' suggest the possibility that cells may utilize similar mechanisms to resist dynamical loads as they do in the case of static loads. Whereas it is clear how geometrical rearrangements of cytoskeletal filaments may come into play in determining the dependence of G' on P, it is not that obvious how they could explain the dependence of G'' on P. A possible explanation for the latter is as follows. In a purely elastic prestressed structure

that is subjected to a harmonic strain excitation, all three mechanisms are in phase with the applied strain as long as the structural response is approximately linear and inertial effects are negligible. Consequently, $G'' \equiv 0$. However, in a structure affected by linear damping, the three mechanisms may not all be in phase with the applied strain. As these mechanisms depend on P, phase lags associated with each of them will also depend on P. Consequently, $G'' \neq 0$ and depends on P. The mathematical description of this argument is as follows.

There have been several attempts to model cell viscoelastic behavior using the cable-and-strut model. Cañadas et al. (2002) and Sultan et al. (2004) used the six-strut tensegrity model (Fig. 6-7a) with viscoelastic Voigt elements instead of elastic cables and with rigid struts to study the creep and the oscillatory responses of the cell, respectively. Their models predicted prestress-dependent viscoelastic properties that are qualitatively consistent with experiments. Sultan et al. (2004) also attempted to quantitatively match model predictions with experimental data. They showed that with a suitable choice of model parameters one can provide a very good quantitative correspondence to the observed dependences of G' and G'' on P (Fig. 6-9). However, this could be accomplished only with a very high degree of inhomogeneity in model parameters (variation of several orders of magnitudes), which is not physically realistic.

The specific issue of time- and rate-of-deformation-dependence in explaining the viscoelastic behavior of cells is covered in Chapters 3, 4 and 5 of this book. However, it will be addressed briefly here in the context of the tensegrity idea. A growing body of evidence indicates that the oscillatory response of various cell types follows a weak power-law dependence on frequency, ω^k where $0 \leq k \leq 1$, over several orders of magnitude of ω (Goldmann and Ezzel, 1996; Fabry et al., 2001; Alcaraz et al., 2003). In the limits when $k = 0$, rheological behavior is Hookean elastic solid-like, and when $k = 1$ it is Newtonian viscous fluid-like. A power-law behavior implies the absence of an internal time scale in the structure. Thus, it rules out the Voigt model, the Maxwell model, the standard linear solid model, and other models with a discrete number of time constants (see for example, Sato et al., 1990; Baush et al., 1998). The power-law behavior observed in cells persists even after cell contractility is altered. The only parameter that changes is the power-law exponent k; in contracted airway smooth muscle cells k decreases, whereas in relaxed cells it increases relative to the baseline (Fabry et al., 2001; Stamenović et al., 2004). Based on these observations, an empirical relationship between k and P has been established (Stamenović et al., 2004). It was found that k decreases approximately logarithmically with increasing P. This result suggests that the cytoskeletal contractile stress regulates the transition between solid-like and fluid-like cell behavior.

The observed relationship between k and P appears not to be an a priori prediction of the tensegrity-based models. Rather, it depends on rheological properties of individual structural members and is rooted in the dynamics (thermal fluctuations) of molecules of the cytoskeleton. These dynamics can lead to a power-law behavior of the entire network (Suki et al., 1994). It is feasible, however, that tensile force carried by prestressed cytoskeletal filaments may influence their molecular dynamics, which in turn may explain why P affects the exponent k in the power-law behavior of cells (Stamenović et al., 2004). This has yet to be shown. Another possibility is that

molecules of the cytoskeleton exhibit highly nonhomogeneous properties that would lead to a wide distribution of time constants, and thereby to a power-law behavior, as shown by Sultan et al. (2004).

In summary, the basic mechanisms of the tensegrity model can explain the dependence of cell viscoelastic properties on the cytoskeletal prestress. These mechanisms cannot completely explain the frequency response of cells, however, which conforms to a power-law. This power-law behavior seems to be primarily determined by rheology of individual cytoskeletal filaments and their own dynamics (thermal fluctuations, and so forth), rather than by structural dynamics of the cytoskeleton.

Conclusion

This chapter has shown that the tensegrity model is a useful approach for studying mechanics of living cells starting from first principles. This approach elucidates how simple structural models naturally come to express many seemingly complex behaviors observed in cells. This does not preclude the numerous chemically and genetically mediated mechanisms (such as, cytoskeletal remodeling, acto-myosin motor kinetics, cross-linking) that are known to regulate cytoskeletal filament assembly and force generation. Rather, it elucidates a higher level of organization in which these events function and may be regulated.

Taken together, results presented in this chapter can be summarized as follows. First, the cytoskeletal prestress is a key determinant of cell deformability. This feature is consistent with all forms of cellular tensegrity models: the cortical membrane model; the cable net model; and the cable-and-strut model. As a consequence, cell stiffness increases with increasing prestress in nearly direct proportion. Second, depending on the cell type and the extent of cell spreading, one may invoke accordingly different types of tensegrity models in order to describe the effect of the prestress on cellular mechanics. Clearly, various types of ad hoc models unrelated to tensegrity may also provide very useful descriptions of cell mechanical behavior under certain experimental conditions (compare Theret et al., 1988; Sato et al., 1990; Forgacs, 1995; Satcher and Dewey, 1996; Bausch et al., 1998; Fabry et al., 2001). However, the studies described here show that the current formulation of the cellular tensegrity model, although highly simplified, embodies many of the key behaviors of cells. Third, the tensegrity model can explain some aspects of cell viscoelastic behavior, but not all. The behavior appears to be primarily related to rheology and molecular dynamics of individual cytoskeletal filaments. Nevertheless, the observed relationship between viscoelastic properties of the cell and cytoskeletal prestress suggests that rheology of individual filaments may be modulated by the prestress through the mechanisms of tensegrity. This is a subject of future studies that will show whether the tensegrity model is useful only in describing and understanding static elastic behavior of cells, or whether it is also useful for describing and understanding cell dynamic viscoelastic behavior.

A long-term goal is to use the tensegrity idea as a mathematical framework to help understand and predict how mechanical and chemical signals interplay to regulate cell function as well as gene expression. In addition, this model may reveal how cytoskeletal structure, prestress, and the extracellular matrix come into play in the

control of cellular information processes (Ingber, 2003b). The biological ground for these applications has already been laid (Ingber 2003a; 2003b). It is the task of bioengineers to carry on this work further.

Acknowledgement

I thank Drs. D. E. Ingber, N. Wang, M. F. Coughlin, and J. J. Fredberg for their collaboration and support in the course of my research of cellular mechanics. Special thanks go to Drs. Ingber and Wang for critically reviewing this chapter.

This work was supported by National Heart, Lung, and Blood Institute Grant HL-33009.

References

Albert-Buehler G (1987) Role of cortical tension in fibroblast shape and movement. *Cell Motil. Cytoskel.*, 7: 54–67.

Alcaraz J, Buscemi L, Grabulosa M, Trepat X, Fabry B, Farre R, Navajas D. (2003) Microrheology of human lung epithelial cells measured by atomic force microscopy. *Biophys. J.*, 84: 2071–2079.

An SS, Laudadio RE, Lai J, Rogers RA, Fredberg JJ (2002) Stiffness changes in cultured airway smooth muscle cells. *Am. J. Physiol. Cell Physiol.*, 283: C792–C801.

Bausch A, Ziemann F, Boulbitch AA, Jacobson K, Sackmann E (1998) Local measurements of viscoelastic parameters of adherent cell surfaces by magnetic bead microrheometry. *Biophys. J.*, 75: 2038–2049.

Boey SK, Boal DH, Discher DE (1998) Simulations of the erythrocyte cytoskeleton at large deformation. I. Microscopic models. *Biophys. J.*, 75: 1573–1583.

Bray D, Heath J, Moss D (1986) The membrane-associated "cortex" of animal cells: Its structure and mechanical properties. *J. Cell Sci. Suppl.*, 4: 71–88.

Brodland GW, Gordon R (1990) Intermediate filaments may prevent buckling of compressively loaded microtubules. *ASME J. Biomech. Eng.*, 112: 319–321.

Budiansky B, Kimmel E (1987) Elastic moduli of lungs. *ASME J. Appl. Mech.*, 54: 351–358.

Burkhardt R (2004) A technology for designing tensegrity domes and spheres. http:www.intergate.com/∼bobwb/ts/prospect/prospect/htm.

Butler JP, Tolić-Nørrelykke IM, Fredberg JJ (2002) Estimating traction fields, moments, and strain energy that cells exert on their surroundings. *Am. J. Physiol. Cell Physiol.*, 282: C595–C605.

Cai S, Pestic-Dragovich L, O'Donnell ME, Wang N, Ingber DE, Elson E, Lanorelle P (1998) Regulation of cytoskeletal mechanics and cell growth by myosin light chain phosphorylation. *Am. J. Physiol.*, *Cell Physiol.*, 275: C1349–C1356.

Cañadas P, Laurent VM, Oddou C, Isabey D, Wendling S (2002) A cellular tensegrity model to analyze the structural viscoelasticity of the cytoskeleton. *J. Theor. Biol.*, 218: 155–173.

Coughlin MF, Stamenović D (1998) A tensegrity model of the cytoskeleton in spread and round cells. *ASME J. Biomech. Eng.*, 120: 770–777.

Coughlin MF, Stamenović D (2003) A prestressed cable network model of adherent cell cytoskeleton. *Biophys. J.*, 84: 1328–1336.

Discher DE, Boal DH, Boey SK (1998) Stimulations of the erythrocyte cytoskeleton at large deformation. II. Micropipette aspiration. *Biophys. J.*, 75: 1584–1597.

Eckes B, Dogic D, Colucci-Guyon E, Wang N, Maniotis A, Ingber D, Merckling A, Langa F, Aumailley M, Delouvée A, Koteliansky V Babinet C, Krieg T (1998) Impaired mechanical stability, migration and contractile capacity in vimentin-deficient fibroblasts. *J. Cell Sci.*, 111: 1897–1907.

Evans E (1983) Bending elastic modulus of red blood cell membrane derived from buckling instability in micropipet aspiration tests. *Biophys. J.*, 43: 27–30.

Evans E, Yeung A (1989) Apparent viscosity and cortical tension of blood granulocytes determined by micropipet aspiration. *Biophys. J.*, 56: 151–160.

Evans E, Leung A, Zhelev D (1993) Synchrony of cell spreading and contraction force as phagocytes engulf large pathogens. *J. Cell Biol.*, 122: 1295–1300.

Fabry B, Maksym GN, Hubmayr RD, Butler JP, Fredberg JJ (1999) Implications of heterogeneous bead behavior on cell mechanical properties measured with magnetic twisting cytometry. *J. Magnetism Magnetic Materials* 194: 120–125.

Fabry B, Maksym GN, Butler JP, Glogauer M, Navajas D, Fredberg JJ (2001) Scaling the microrheology of living cells. *Phys. Rev. Lett.*, 87: 148102(1–4).

Forgacs G (1995) On the possible role of cytoskeletal filamentous networks in intracellular signaling: An approach based on percolation. *J. Cell Sci.*, 108: 2131–2143.

Fredberg JJ, Jones KA, Nathan M, Raboudi S, Prakash YS, Shore SA, Butler JP, Sieck GC (1996) Friction in airway smooth muscle: Mechanism, latch, and implications in asthma. *J. Appl. Physiol.*, 81: 2703–2712.

Fuller B (1961) Tensegrity. *Portfolio Artnews Annual* 4: 112–127.

Fung YC (1993) *Biomechanics – Mechanical Properties of Living Tissues*, 2nd edition. New York, Springer.

Fung YC, Liu SQ (1993) Elementary mechanics of the endothelium of blood vessels. *ASME J. Biomech. Eng.*, 115: 1–12.

Gittes F, Mickey B, Nettleton J, Howard J (1993) Flexural rigidity of microtubules and actin filaments measured from thermal fluctuations in shape. *J. Cell Biol.*, 120: 923–934.

Goldmann, WH, Ezzel, RM (1996) Viscoelasticity of wild-type and vinculin deficient (5.51) mouse F9 embryonic carcinoma cells examined by atomic force microscopy and rheology. *Exp. Cell Res.*, 226: 234–237.

Harris AK, Wild P, Stopak D (1980) Silicon rubber substrata: A new wrinkle in the study of cell locomotion. *Science*, 208: 177–179.

Heidemann SR, Buxbaum RE (1990) Tension as a regulator and integrator of axonal growth. *Cell Motil. Cytoskel.*, 17: 6–10.

Heidemann SR, Kaech S, Buxbaum RE, Matus A (1999) Direct observations of the mechanical behavior of the cytoskeleton in living fibroblasts. *J. Cell Biol.*, 145: 109–122.

Helmke BP, Rosen AB, Davies PF (2003) Mapping mechanical strain of an endogenous cytoskeletal network in living endothelial cells. *Biophys. J.*, 84: 2691–2699.

Hu S, Chen J, Fabry B, Namaguchi Y, Gouldstone A, Ingber DE, Fredberg JJ, Butler JP, Wang N (2003) Intracellular stress tomography reveals stress and structural anisotropy in the cytoskeleton of living cells. *Am. J. Physiol. Cell Physiol.*, 285: C1082–C1090.

Hu S, Chen, J, Wang N (2004) Cell spreading controls balance of prestress by microtubules and extracellular matrix. *Frontiers in Bioscience*, 9: 2177–2182.

Hubmayr RD, Shore SA, Fredberg JJ, Planus E, Panettieri Jr, RA, Moller W, Heyder J, Wang N (1996) Pharmacological activation changes stiffness of cultured human airway smooth muscle cells. *Am. J. Physiol. Cell Physiol.*, 271: C1660–C1668.

Ingber DE (1993) Cellular tensegrity: Defining new rules of biological design that govern the cytoskeleton. *J. Cell Sci.*, 104: 613–627.

Ingber DE (2003a) Cellular tensegrity revisited I. Cell structure and hierarchical systems biology. *J. Cell Sci.*, 116: 1157–1173.

Ingber DE (2003b) Tensegrity II. How structural networks influence cellular information-processing networks. *J. Cell Sci.*, 116: 1397–1408.

Ingber DE, Jameison JD (1985) Cells as tensegrity structures: Architectural regulation of histodifferentiation by physical forces transduced over basement membrane. In: *Gene Expression during Normal and Malignant Differentiation*. (eds. Anderson LC, Gahmberg GC, Ekblom P), Orlando, FL: Academic Press, pp. 13–32.

Ingber DE, Madri, JA, Jameison JD (1981) Role of basal lamina in the neoplastic disorganization of tissue architecture. *Proc. Nat. Acad. Sci. USA*, 78: 3901–3905.

Ingber DE, Heidemann SR, Lamoroux P, Buxbaum RE (2000) Opposing views on tensegrity as a structural framework for understanding cell mechanics. *J. Appl. Physiol.*, 89: 1663–1670.

Ishijima A, Kojima H, Higuchi H, Harada Y, Funatsu T, Yanagida T (1996) Multiple- and single-molecule analysis of the actomyosin motor by nanometer-piconewton manipulation with a microneedle: Unitary steps and forces. *Biophys. J.*, 70: 383–400.

Kaech S, Ludin B., Matus A (1996) Cytoskeletal plasticity in cells expressing neuronal microtubule-expressing proteins. *Neuron*, 17: 1189–1199.

Kolodney MS, Wysolmerski RB (1992) Isometric contraction by fibroblasts and endothelial cells in tissue culture: A quantitative study. *J. Cell Biol.*, 117: 73–82.

Kolodney MS, Elson EL (1995) Contraction due to microtubule disruption is associated with increased phosphorylation of myosin regulatory light chain. *Proc. Natl. Acad. Sci. USA*, 92: 10252–10256.

Kurachi M, Masuki H, Tashiro H (1995) Buckling of single microtubule by optical trapping forces: Direct measurement of microtubule rigidity. *Cell Motil. Cytoskel.*, 30: 221–228.

MacKintosh FC, Käs J, Janmey PA (1995) Elasticity of semiflexible biopolymer networks. *Phys. Rev. Lett.*, 75: 4425–4428.

Maniotis AJ, Chen CS, Ingber DE (1997) Demonstration of mechanical connectivity between integrins, cytoskeletal filaments, and nucleoplasm that stabilize nuclear structure. *Proc. Natl. Acad. Sci. USA*, 94: 849–854.

Mehta D, Gunst SJ (1999) Actin polymerization stimulated by contractile activation regulates force development in canine tracheal smooth muscle. *J. Physiol.* (*Lund.*), 519: 829–840.

Mijailovich SM, Butler JP, Fredberg JJ (2000) Perturbed equilibrium of myosin binding in airway smooth muscle: Bond-length distributions, mechanics, and ATP metabolism. *Biophys. J.*, 79: 2667–2681.

Mijailovich SM, Kojic M, Zivkovic M, Fabry B, Fredberg JJ (2002) A finite element model of cell deformation during magnetic bead twisting. *J. Appl. Physiol.*, 93: 1429–1436.

Paul RJ, Bowman P, Kolodney MS (2000) Effects of microtubule disruption on force, velocity, stiffness and $[Ca^{2+}]_i$ in porcine coronary arteries. *Am. J. Physiol. Heart Circ. Physiol.*, 279: H2493–H2501.

Pelham RJ, Wang YL (1997) Cell locomotion and focal adhesions are regulated by substrate flexibility. *Proc. Natl. Acad. Sci. USA*, 94: 13661–13665.

Petersen NO, McConnaughey WB, Elson EL (1982) Dependence of locally measured cellular deformability on position on the cell, temperature, and cytochalasin B. *Proc. Natl. Acad. Sci. USA*, 79: 5327–5331.

Porter KR (1984) The cytomatrix: A short history of its study. *J. Cell Biol.*, 99: 3s–12s.

Pourati J, Maniotis A, Spiegel D, Schaffer JL, Butler JP, Fredberg JJ, Ingber DE, Stamenović D, Wang N (1998) Is cytoskeletal tension a major determinant of cell deformability in adherent endothelial cells? *Am J. Physiol. Cell Physiol.*, 274: C1283–C1289.

Satcher RL Jr, Dewey CF Jr (1996) Theoretical estimates of mechanical properties of the endothelial cell cytoskeleton. *Biophys. J.*, 71: 109–118.

Satcher R, Dewey CF Jr, Hartwig JH (1997) Mechanical remodeling of the endothelial surface and actin cytoskeleton induced by fluid flow. *Microcirculation*, 4: 439–453.

Sato M, Theret DP, Wheeler LT, Ohshima N, Nerem RM (1990) Application of the micropipette technique to the measurements of cultured porcine aortic endothelial cell viscoelastic properties. *ASME J. Biomech. Eng.*, 112: 263–268.

Schmid-Schönbein GW, Kosawada T, Skalak R, Chien S (1995) Membrane model of endothelial cell and leukocytes. A proposal for the origin of cortical stress. *ASME J. Biomech. Eng.*, 117: 171–178.

Sims JR, Karp S, Ingber DE (1992) Altering the cellular mechanical force balance results in integrated changes in cell, cytoskeletal and nuclear shape. *J. Cell Sci.*, 103: 1215–1222.

Stamenović D (1990) Micromechanical foundations of pulmonary elasticity. *Physiol. Rev.*, 70: 1117–1134.

Stamenović D (2005) Microtubules may harden or soften cells, depending on the extent of cell distension. *J. Biomech.*, 38:1728–1732.

Stamenović D, Ingber DE (2002) Models of cytoskeletal mechanics of adherent cells. *Biomech. Model Mechanobiol.*, 1: 95–108.

Stamenović D, Fredberg JJ, Wang N, Butler JP, Ingber DE (1996) A microstructural approach to cytoskeletal mechanics based on tensegrity. *J. Theor. Biol.*, 181: 125–136.

Stamenović D, Mijailovich SM, Tolić-Nørrelykke IM, Chen J, Wang N (2002a) Cell prestress. II. Contribution of microtubules. *Am. J. Physiol. Cell Physiol.*, 282: C617–C624.

Stamenović D, Liang Z, Chen J, Wang N (2002b) The effect of cytoskeletal prestress on the mechanical impedance of cultured airway smooth muscle cells. *J. Appl. Physiol.*, 92: 1443–1450.

Stamenović D, Suki B, Fabry B, Wang N, Fredberg JJ (2004) Rheology of airway smooth muscle cells is associated with cytoskeletal contractile stress. *J. Appl. Physiol.*, 96: 1600–1605.

Suki B, Barabási A-L, Lutchen KR (1994) Lung tissue viscoelasticity: A mathematical framework and its molecular basis. *J. Appl. Physiol.*, 76: 2749–2759.

Sultan C, Stamenović D, Ingber DE (2004) A computational tensegrity model predicts dynamic rheological behaviors in living cells. *Ann. Biomed. Eng.*, 32: 520–530.

Tang D, Mehta D, Gunst SJ (1999) Mechanosensitive tyrosine phosphorylation of paxillin and focal adhesion kinase in tracheal smooth muscle. *Am. J. Physiol. Cell Physiol.*, 276: C250–C258.

Theret DP, Levesque MJ, Sato M, Nerem RM, Wheeler LT (1988) The application of a homogeneous half-space model in the analysis of endothelial cell micropipette measurements. *ASME J. Biomech. Eng.*, 110: 190–199

Timoshenko SP, Gere JM (1988) *Theory of Elastic Stability*. New York: McGraw-Hill.

Tolić-Nørrelykke IM, Butler JP, Chen J, and Wang N (2002) Spatial and temporal traction response in human airway smooth muscle cells. *Am J Physiol. Cell Physiol.*, 283, C1254–C1266.

Volokh, KY, Vilnay O (1997) New cases of reticulated underconstrained structures. *Int J Solids Structures* 34: 1093–1104.

Volokh KY, Vilnay O, Belsky M (2000), Tensegrity architecture explains linear stiffening and predicts softening of living cells. *J. Biomech.*, 33: 1543–1549.

Wang N (1998) Mechanical interactions among cytoskeletal filaments. *Hypertension*, 32: 162–165.

Wang N, Ingber DE (1994) Control of the cytoskeletal mechanics by extracellular matrix, cell shape, and mechanical tension. *Biophys. J.*, 66: 2181–2189.

Wang N, Stamenović D (2000) Contribution of intermediate filaments to cell stiffness, stiffening and growth. *Am. J. Physiol. Cell Physiol.*, 279: C188–C194.

Wang N, Butler JP, Ingber DE (1993) Mechanotransduction across cell surface and through the cytoskeleton. *Science*, 26: 1124–1127.

Wang N, Naruse K, Stamenović D, Fredberg JJ, Mijailovich SM, Tolić-Nørrelykke IM, Polte T, Mannix R, Ingber DE (2001) Mechanical behavior in living cells consistent with the tensegrity model. *Proc. Natl. Acad. Sci. USA*, 98: 7765–7770.

Wang N, Tolić-Nørrelykke IM, Chen J, Mijailovich SM, Butler JP, Fredberg JJ, Stamenović D (2002) Cell prestress. I. Stiffness and prestress are closely associated in adherent contractile cells. *Am. J. Physiol. Cell Physiol.*, 282: C606–C616.

Waterman-Storer CM, Salmon ED (1997) Actomyosin-based retrograde flow of microtubules in lamella of migrating epithelial cells influences microtubule dynamic instability and turnover and is associated with microtubule breakage and treadmilling. *J. Cell Biol.*, 139: 417–434.

Wendling S, Oddou C, Isabey D (1999) Stiffening response of a cellular tensegrity model. *J. Theor. Biol.*, 196: 309–325.

Yanagida T, Nakase M, Nishiyama K, Oosawa F (1984) Direct observations of motion of single F-actin filaments in the presence of myosin. *Nature*, 307: 58–60.

Zhelev DV, Needham D, Hochmuth RM (1994) Role of the membrane cortex in neutrophil deformation in small pipettes. *Biophys. J.*, 67: 696–705.